



LJMU Research Online

Rivera Quiroga, R, Cardona, N, Padilla, L, Rivera, W, Rocha Roa, C, Diaz, M, Morales, S and Martinez, M

In silico selection and in vitro evaluation of new molecules that inhibit the adhesion of Streptococcus mutans through Antigen I/II

<http://researchonline.ljmu.ac.uk/id/eprint/14149/>

Article

Citation (please note it is advisable to refer to the publisher's version if you intend to cite from this work)

Rivera Quiroga, R, Cardona, N, Padilla, L, Rivera, W, Rocha Roa, C, Diaz, M, Morales, S and Martinez, M In silico selection and in vitro evaluation of new molecules that inhibit the adhesion of Streptococcus mutans through Antigen I/II. International Journal of Molecular Sciences. ISSN 1422-0067

LJMU has developed **LJMU Research Online** for users to access the research output of the University more effectively. Copyright © and Moral Rights for the papers on this site are retained by the individual authors and/or other copyright owners. Users may download and/or print one copy of any article(s) in LJMU Research Online to facilitate their private study or for non-commercial research. You may not engage in further distribution of the material or use it for any profit-making activities or any commercial gain.

The version presented here may differ from the published version or from the version of the record. Please see the repository URL above for details on accessing the published version and note that access may require a subscription.

For more information please contact researchonline@ljmu.ac.uk

<http://researchonline.ljmu.ac.uk/>



1 Article

2 *In silico selection and in vitro evaluation of new*
3 *molecules that inhibit the adhesion of Streptococcus*
4 *mutans through Antigen I/II*
5

6 Raúl E. Rivera-Quiroga^{1,2*}, Néstor Cardona¹, Leonardo Padilla², Wbeimar Rivera³, Cristian Rocha-
7 Roa⁴, Mayri A. Diaz De Rienzo ⁵, Sandra M. Morales³, María C. Martínez³
8

9 ¹ Faculty of dentistry, Antonio Nariño University. Group of Investigation in oral Health. Av. Bolívar # 49 North
10 – 30, Armenia – Quindío (Zip Code: 630001), Colombia; Raul Eduardo Rivera - rriveraquiroya@uan.edu.co.
11 Nestor Ivan Cardona - nestorcardonape@uan.edu.co.
12

13 ² Faculty of Health Sciences, Quindío University, GYMOL Group street 12N, Armenia, Quindío (Zip Code:
14 630001), Colombia. lpadilla@uniquindio.edu.co
15

16 ³ Faculty of Dentistry, University of Antioquia, Oral Microbiology Laboratory, 64 Street No. 52-59, Block 31,
17 No. 216, Health Area, Medellín – Antioquia (Zip Code: 050001) Colombia. Wbeimar Rivera -
18 wbeimar.rivera@udea.edu.co. Sandra Milena Morales - sandra.morales@udea.edu.co. Maria Cecilia
19 Martinez - mcecilia.martinez@udea.edu.co.
20

21 ⁴ Faculty of Health Sciences, Quindío University, GEPAMOL Group street 12N, Armenia, Quindío (Zip Code:
22 630001), Colombia. ccrochar@uqvirtual.edu.co.
23

24 ⁵ School of Pharmacy and Biomolecular Sciences, Liverpool John Moores University, James Parsons Building
25 10.05C, Byrom Street, Liverpool (Zip Code: L3 3AF), United Kingdom. m.a.diaz@ljmu.ac.uk.
26

27 * Correspondence: Raul Eduardo Rivera Quiroga, Group of Investigation in Oral Health, Faculty of Dentistry,
28 Antonio Nariño University, Av. Bolívar # 49 North-30, Armenia, Quindío 630001, Colombia. Tel/Fax:
29 +573128693374/+5767494981, E-mail: rriveraquiroya@uan.edu.co.
30

Received: date; Accepted: date; Published: date

31 **Abstract:** *Streptococcus mutans* is the main early colonizing cariogenic bacteria because it recognizes
32 salivary pellicle receptors. The Antigen I/II of *S. mutans* is one of the most important adhesins in this
33 process, is involved in the adhesion to the tooth surface and the bacterial co-aggregation in the early
34 stage of biofilm formation. However, this protein has not been used as a target in a virtual strategy
35 search for inhibitors. Based on the predicted binding affinities, drug-like properties and toxicity,
36 molecules were selected and evaluated for their ability to reduce *S. mutans* adhesion. A virtual
37 screening of 883,551 molecules was conducted, cytotoxicity analysis on fibroblast cells, *S. mutans*
38 adhesion studies, scanning electron microscopy analysis for bacterial integrity and molecular
39 dynamics simulation were also performed. We have found three molecules (ZI-187, ZI-939, ZI-906)
40 without cytotoxic activity, which inhibited about 90% the adhesion of *S. mutans* to polystyrene
41 microplates. Molecular dynamic simulation by 300 nanoseconds showed stability of the interaction
42 between ZI-187 and Ag I/II (PDB: 3IPK). This work provides new molecules that targets Ag I/II and
43 have the capacity to inhibit *in vitro* the *S. mutans* adhesion on polystyrene microplates.

44 Key words: (*Streptococcus mutans*, adhesion proteins, Antigen I/II, dental caries, Structure-based
45 virtual screening, molecular dynamics)

46 1. Introduction

47 In 2016 dental caries was classified as the most prevalent pathology in the world, affecting 2.4
48 billion people [1,2]. This pathology is one of the oral diseases related to the oral microbiota alteration
49 [3], characterized by perforations or structural damage of the teeth, called carious lesions [4]. There
50 are three well-known risk factors for the development of caries: personal factors that are related to
51 socioeconomic status i.e., dental insurance coverage, attitudes and knowledge about oral health and
52 oral hygiene; oral environmental factors such as saliva, fluoride, chewing gum, pH, bacteria, calcium,
53 phosphates, proteins and factors that directly contribute to the development of caries, like, the tooth,
54 diet (consumption of sugars), bacterial biofilms and time [5].
55

56 Oral microorganisms that cannot adhere to a surface are transported by salivary flow out of the
57 mouth and into the digestive tract, but many oral bacteria possess mechanisms of adherence to solid
58 surfaces (co-adhesion), such as coated teeth from salivary films, to squamous surfaces such as
59 epithelial tissue or bacteria that are attached to the surface (co-aggregation) [6]. The streptococci
60 compete for adhesion binding sites on the saliva-coated tooth surface and are able to produce
61 antimicrobial compounds and *S.mutans* can become dominant in oral biofilms, leading to dental
62 caries development [7]. This organism also produces glycosyltransferases (gtfs), multiple glucan-
63 binding proteins (Gbps), antigen I/II (also called SpaP, Pac, P1), and collagen-binding protein, these
64 surface proteins coordinate the production of dental plaque [8]. The ability to form biofilms is one of
65 the main *S. mutans* characteristics and it is a complex process of protein–bacterium interaction that
66 begins with the attachment of a single cell, aggregation, microcolony formation until a mature biofilm
67 [9]. Adherence to host tissues represents a critical step in the pathogenic process and is usually
68 mediated by bacterial surface-exposed proteins in which *S. mutans* have mechanisms for adhesion
69 sucrose-dependent (Gtfs essential) and sucrose-independent (Ag I/II essential) [10].
70

71 In the absence of sucrose, *S. mutans* synthesizes several important adhesins such as antigen I/II
72 (also called SpaP, Pac), which specifically binds to a glycoprotein called SAG (salivary agglutinin)
73 [11,12], which has been proposed that participates as well in the tooth bacterial adhesion [13], and
74 biofilm formation, this due to the fact that Ag I/II-deficient mutants formed 65% less biofilm than the
75 wild-types [14] and a decrease in its ability to promote the aggregation and invasion of the dentin
76 of the collagen-dependent tooth [8,14]. Ag I/II virulence has been evaluated in a gnotobiotic rat model
77 [15] and has been considered a promising target antigen for anticaries vaccines [16–19]. The overall
78 structure of antigen I/II is conserved in all members of this protein family, this multidomain protein
79 is composed of 1500–1566 amino acid residues (140- to 180-kDa) with a structure composed of
80 alanine-rich variable V, proline-rich P, and C-terminal C domains [19–21]. The antigen I/II family of
81 adhesins are cell wall-associated polypeptides that are widely distributed on the cell surface of many
82 streptococci and is not only important for initial streptococcal adhesion to the host, but also for inter-
83 bacterial adhesion and “secondary” colonization; it also mediates interactions between *S. mutans* and
84 *Candida albicans* [22,23]. Additionally, the presence of these protein on the cell surface determines the
85 adherence of *S. mutans* to SAG but no difference in SAG-mediated adherence could be seen between
86 type A and B strains [24]. Analysis of host and bacterial phenotype variation in adhesion of *S.mutans*
87 has determined that the host saliva phenotype and Ag I/II V-region plays a prominent role [25].
88 However, crystal structure information shows a possible model for AgI/II binding to SAG, where
89 interactions occur at both the distal end through the A3VP1 region, and at a secondary adherence site
90 mediated by the C-terminal domain [20].
91

92 Numerous therapies for dental caries, have been proposed apart from the extensive use of
93 fluoride, as xylitol [26,27], chlorhexidine [28,29], immunization [16,30], molecules derived from
94 natural products [31], metal ions or oxidizing agents and even antibodies that specifically bind to *S.*

95 *mutans* targets (GtfB, GtfC, GtfD, Ag I/II) inhibiting the bacterial ability to develop biofilms [18,32],
96 such strategies have been reported to target specific caries pathogens or to indiscriminately eliminate
97 oral microbiota. However, the effectiveness of these methods is yet to be recognized, and safety
98 concerns have been raised with regard to their negative impact in the ecology of the oral microbiota
99 [33]. Other potential anticariogenic methods include the casein phosphopeptide-amorphous calcium
100 phosphate nanocomplex (CPP-ACP), an agent that saturates saliva and biofilm, favoring the dental
101 remineralization [34]; arginine which inhibit the growth of acidogenic or aciduric bacteria by raising
102 the pH of the oral environment sugar substitutes [33] it has been proposed that the combined
103 antimicrobial effect of arginine and fluoride have a potential synergistic effect in maintaining an eco-
104 friendly oral microbial equilibrium which helps prevent tooth decay, though the mechanism of
105 arginine over the destabilization of biofilm is not yet clear [35,36]. These promising approaches may
106 include the use of arginine as prebiotic and selected bacterial strains with arginine deiminase
107 pathway (ADS+) as probiotic, like *Streptococcus dentisani* a bacterial isolated from dental plaque of
108 caries-free individuals that has been shown to have several beneficial effects *in vitro* which could
109 contribute to promote oral health, including an antimicrobial activity against oral pathogens by the
110 production of bacteriocins and a pH buffering capacity through ammonia (Produced by arginine
111 deiminase system) and the topic application of these probiotic could decrease the amount of dental
112 plaque, but no differences were observed in the placebo group [37].
113

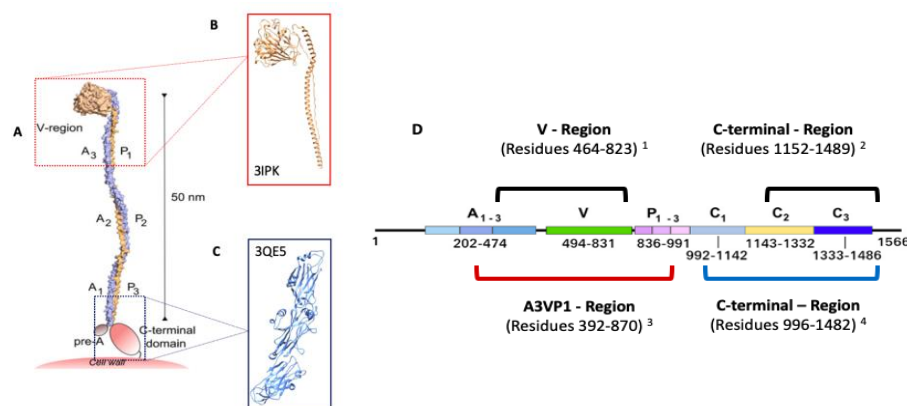
114 Few of these treatments have been proven to confer selectivity against *S. mutans* or other
115 cariogenic bacteria to prevent caries without disturbing the ecological balance between pathogens
116 and commensal bacteria in the oral cavity. In recent decades, the virtual search for inhibitors based
117 on structures has taken interest in drug discovery [38–40]; for oral microbiology the use of this
118 strategy is relatively new, particularly in the cariogenic context, but several proteins have been
119 proposed that could be used as inhibitory molecules [41]. Gtf-C has been used as a target on the
120 search of molecules with affinity to this protein and for selectively inhibition of *S. mutans* biofilms
121 formation mainly due to the ability to inhibit the synthesis of exopolysaccharides (EPS) *in vitro*, the
122 biofilm formation and reduce *in vivo* the caries incidence and severity in a rat model [42,43]. Although
123 the Ag I/II adhesin has been reported to play an important in the early stages of *S. mutans* biofilm
124 development, participating in adhesion and co-aggregation with other bacteria and fungi such as *C.*
125 *albicans*, there are no reports of computational studies that use this protein as target, therefore, the
126 aim of this work is to identify *in silico* molecules with inhibitory effect on *S. mutans* Ag I/II, , which
127 have no cytotoxic activity on human cells.

128 2. Results and Discussion

129 2.1. Structure based virtual Screening

130 2.1.1. Target proteins selection

131 The Ag I/II of *S. mutans* play an essential role in the etiology and pathogenesis of dental caries.
132 Therefore, the discovery of inhibitors of Ag I/II may facilitate the development of drugs that prevent
133 dental caries. Ag I/II is one of the cell wall-anchored adhesins that mediates attachment of *S. mutans*
134 to tooth surfaces, recognize salivary glycoproteins, and are also involved in biofilm formation.
135 Finding small-molecule that bind to the Ag I/II may interfere with the function of these adhesine. To
136 address this, we selected a sequence of the *S. mutans* Ag I/II adhesin and we found a crystal structure
137 from different regions of AgI/II, which corresponds to the A3VP1 region (PDB: 3IPK) [21], C-terminal
138 domain, region V (PDB: 1JMM) [44] and two from the C-terminal domain (PDB: 3QE5) [20] and (PDB:
139 3OPU) [45] (Figure S1). According to sequence similarity and coverage results (Table S1), the crystals
140 structures of the proteins 3IPK and 3QE5 were selected, due to their role in *S. mutans* adhesion to the
141 tooth, through their SAG binding [21] (Figure 1).



142

143

144 **Figure 1.** Crystals structures from the *S. mutans* Ag I/II protein (A). Model of *S. mutans* Ag I/II structure and
 145 predicted binding with human SAG (taken from [21]). (B) Crystal structure of A3VP1 protein from Ag I/II (3IPK)
 146 [21]. (C). Crystal structure C-domain protein from the Ag I/II (3QE5) [20]. (D). Schematic representation of the
 147 Ag I/II protein sequence (1566 aa) and the description of the aa residues that constitute the crystals structures of
 148 the protein regions: 1- Region V (PDB: 1JMM) [44]; 2- C-terminal domain [45]; 3- A3VP1 region (PDB: 3IPK) [21]
 149 and 4- the C-terminal region (PDB: 3QE5) [20].

150 Sequence and structural similarity analysis of 3IPK and 3QE5 was performed in order to identify
 151 other similar proteins in another organism. However, no significant homologies were found, which
 152 could be an indication that these molecules would not affect human (Table S2) or bacterial proteins
 153 important for the ecological balance of the oral microbiota, but a lack of overall protein similarity
 154 may not exclude local similarities in the properties of the ligand binding pockets i.e. two unrelated
 155 proteins may share pockets with the ability to bind a common compound. On the other hand, we
 156 have found sequence homologies with proteins from 23 bacterial species, which are mostly normal
 157 inhabitants of the oral cavity, gastrointestinal and genitourinary tracts, but are associated with
 158 different pathologies (Table S3, S4). Regarding the structural homologies for 3IPK and 3QE5 proteins,
 159 there were no similarities with any human or bacterial proteins, only with *S. mutans* Ag I/II regions,
 160 A3VP1 region (PDB: 3ioxA) [21] and N-terminal and C-terminal interaction complex (PDB: 4tshA)
 161 (Table S5) [46].

162 A fundamental step for the search of molecules based on virtual structures, is the pocket
 163 selection, these sites must have typical characteristics such as concave, have a variety of hydrogen
 164 bridge donors and acceptors and hydrophobic characteristics [47], otherwise, false negatives may
 165 occur when selecting molecules for *in vitro* assays, since errors may occur when there are no binding
 166 sites in the protein or when homology models are used, causing for example, small-volume pockets
 167 to be selected that will generate incorrect unions or conformations [48]. For that reason, in this study,
 168 two multiservers or specific programs were used for protein ligand binding site prediction, which
 169 have different selection algorithms, the MetaPocket uses a consensus method based on the predicted
 170 sites of four free access programs LIGSITEcs, PASS, Q-SiteFinder and SURFNET, which are
 171 combined to improve the success rate of the prediction and which is based on the geometry and
 172 surface of the proteins [49], unlike the COACH that uses the consensus of two methods, one based
 173 on the comparison of specific binding substructures (TM-SITE) and the other on the alignment of the
 174 sequence profile (S-SITE), for predictions of binding sites based on known proteins [50] (Figure S2).

175 2.1.2. Molecules selection

176 Ten molecules were arbitrarily selected according to their molecular docking score and ten
 177 according to the number of pockets interaction. The lowest docking score indicates high affinity
 178 between the molecule and the ligand. Therefore, molecules that interacted in several binding sites
 179 were selected, because those could have a greater coating of the target protein allowing the inhibition

180 of the two important regions of Ag I/II involved in its adhesin function. Interestingly, we found
 181 molecules that binding to more than one site of the same protein domain, A3VP1 in the V region and
 182 C-terminal region, this could have been possible because these proteins have several conserved
 183 regions in their structure, in PDB: 3IPK the A region typically consists of 3–4 alanine rich repeats (82
 184 residues each) with 23–30% alanine content, the P region has 3–4 proline-rich repeats (39 residues
 185 each) with ~35% proline content and in PDB: 3QE5 the sequence have a high proline content that
 186 forms a repetitive proline- rich region [20,21,51]. In addition, A3VP1 and the C-terminal fragments
 187 has multiple binding sites and similar affinities for binding to SAG, which support the simple model
 188 proposed about the high-affinity binding of AgI/II with SAG occurs via the apical fishhook-like
 189 structure observed within A3VP1, and an additional interaction occurring within the C- terminal
 190 region[21].

191

192

193 **Table 1.** Energy interaction data obtained from recoupling using Autodock Vina with an exhaustiveness
 194 of twenty for the 3IPK and 3QE5 proteins with the selected molecules, molecule libraries and number of pockets
 195 in which each molecule interacted. The molecule highlighted in black was the only one that interacted with high
 196 affinity in different sites in both 3IPK and 3QE5 proteins. COA: COACH program. MET: Metapocket 2.0
 program. Values highlighted in light blue represent the lowest interaction energy values.

| NUMBER OF MOLECULES INTERACTION POCKETS | MOLECULES | LIBRARY | 3IPK | | | | | | 3QE5 | | | | | |
|---|--------------|---------|-------|-------|-------|------|-------|-------|-------|-------|-------|------|-------|------|
| | | | P1 | | P2 | | P3 | | P1 | | P2 | | P3 | |
| | | | COACH | MET | COACH | MET | COACH | MET | COACH | MET | COACH | MET | COACH | MET |
| Not applicable | ZINC68568370 | NAT | -12,8 | -12,8 | -7,5 | -9 | -9,4 | -10,9 | -8,5 | -8,8 | -8,1 | -8,9 | -7,1 | -7,7 |
| | ZINC70669788 | NAT | -11,4 | -12,8 | -7,5 | -8,4 | -8,7 | -10,1 | -7,9 | -8,7 | -7,7 | -7,6 | -7,6 | -6,5 |
| | ZINC70669789 | NAT | -11,5 | -12,7 | -7,3 | -8,3 | -8,8 | -9,8 | -8,1 | -9 | -7,9 | -7,8 | -7,8 | -6,3 |
| | ZINC34257514 | NAT | -12,6 | -12,6 | -6,7 | -8,8 | -7,7 | -9,8 | -6,9 | -8,7 | -6,8 | -7,6 | -6,7 | -7,6 |
| | ZINC04817561 | NAT | -10,3 | -12,4 | -10,1 | -8,3 | -8,6 | -12,4 | -7,2 | -9,2 | -7,1 | -7,9 | -7,2 | -7 |
| | ZINC67912808 | NAT | -12,3 | -12,5 | -8,2 | -8,8 | -8,4 | -9,1 | -7,6 | -9,5 | -7,6 | -8,1 | -7,1 | -6,8 |
| | ZINC70686498 | NAT | -12,2 | -12,2 | -7,8 | -8,2 | -8 | -9,9 | -7,4 | -8,1 | -7,3 | -9,6 | -6,6 | -7,1 |
| | ZINC04015296 | NAT | -11,7 | -11,6 | -8,4 | -9,8 | -9 | -11,7 | -9,3 | -11,4 | -7,5 | -9,3 | -7,4 | -9,8 |
| | ZINC08594547 | LRG | -11,6 | -11,7 | -7,7 | -8,5 | -8,1 | -11,4 | -7,6 | -8,6 | -7,1 | -8,2 | -6,5 | -8,3 |
| 12 | ZINC00970517 | SM | -9,4 | -9,4 | -9 | -8,2 | -7 | -9 | -6,7 | -7,7 | -6,3 | -7,5 | -5,9 | -7,3 |
| 12 | ZINC01033612 | SM | -9,3 | -9,5 | -8,7 | -7,7 | -7,3 | -9,4 | -7,4 | -7,8 | -7 | -8,1 | -7,4 | -7,5 |
| 12 | ZINC08647964 | SM | -9,7 | -9,8 | -9,4 | -7,9 | -7,4 | -10,4 | -6,9 | -8,4 | -6,8 | -8,7 | -6,2 | -7,5 |
| 12 | ZINC12369546 | SM | -9,5 | -10 | -9,1 | -8,3 | -7,5 | -9,8 | -7,9 | -8,3 | -6,7 | -7,8 | -6,8 | -8,5 |
| 12 | ZINC19924906 | SM | -11,1 | -11 | -7,2 | -8,2 | -7,1 | -9,2 | -6,9 | -8,3 | -6,7 | -7,5 | -6,8 | -7,5 |
| 12 | ZINC03120327 | SM | -9,6 | -9,7 | -10,1 | -7,9 | -7,1 | -10,1 | -6,7 | -8 | -7,1 | -8 | -6,9 | -8,5 |
| 12 | ZINC19835160 | SM | -10,3 | -9,5 | -6,9 | -8,7 | -7,7 | -9,7 | -6,6 | -8,4 | -6,7 | -8 | -5,8 | -6,9 |
| 12 | ZINC19835187 | SM | -10,7 | -10,7 | -9,2 | -8,8 | -8,5 | -10,3 | -8,1 | -8,7 | -7,5 | -8,4 | -6,9 | -8,8 |
| 12 | ZINC19924939 | SM | -10,4 | -10,4 | -9 | -8,9 | -7,2 | -8,1 | -7,6 | -7,5 | -7,1 | -8 | -6,4 | -7,9 |
| 12 | ZINC59608258 | SM | -9,4 | -10,1 | -7,8 | -7,9 | -7,2 | -8,9 | -6,8 | -7,7 | -6,1 | -7,6 | -6,3 | -6,7 |

197

198

199

200

201

202

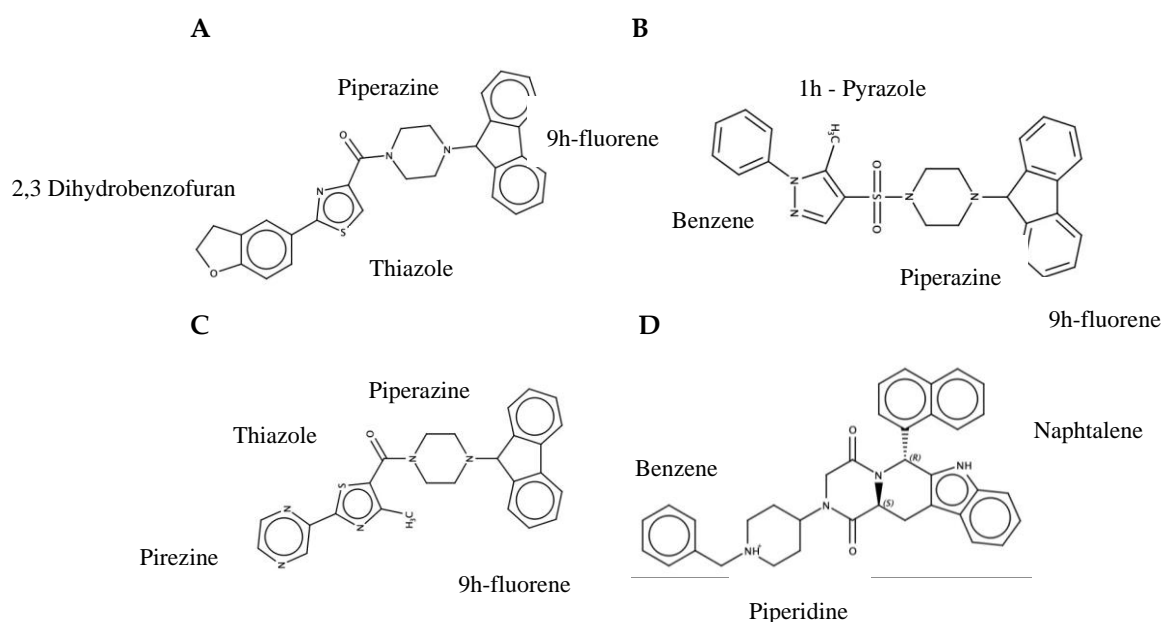
Finally, nineteen molecules were obtained, because the ZINC19924906 molecule from the library "Small" was selected according to the best docking score and the interaction with different ligand sites in the domains. The molecules with the lowest docking score were from the library "Natural", such as ZINC68568370 with a docking score of -12.8. The molecules that had a higher number of binding sites were found from the library "Small" and were coupled to the 12 pockets used for

203 docking, which means that they have affinity for several pockets in both the PDB domain: 3IPK and
 204 PDB: 3QE5 (Table 1).

205 Molecules that comply the standard physical-chemical parameters and pharmacokinetic profiles
 206 are presented in table S6. However, one molecule was discarded for having an LD50 = 10mg / kg (C-
 207 II) (Figure S3) and fourteen for having the probability of presenting hepatotoxicity, carcinogenicity,
 208 immunotoxicity and/or mutagenicity characteristics (Figure S4). Finally, we obtained four molecules
 209 ZINC19835187 (ZI-187), ZINC19924939 (ZI-939), ZINC19924906 (ZI-906) and ZINC70686498 (ZI-498)
 210 (Figure 2) which did not present any probability of cytotoxic characteristics, as well as the
 211 Chlorhexidine (Figure S4).

212

213



214

215

216

217

218

219 **Figure 2.** Molecules structures selected by *in silico* analysis, which have affinity for Ag I/II and
 220 inhibitory potential of *S. mutans* adhesion. **A-** ZI-187; **B-** ZI-939; **C-** ZI-906; **D-** ZI-498.

221 Three molecules belonging to the small library (ZI-187, ZI-939, ZI-906) were selected, molecules
 222 from this library, basically, contain drug-like properties such as molecular weight (<500 Da),
 223 hydrogen bond acceptors (HBA) (<10), hydrogen bond donors (HBD) (<5), partition coefficient AlogP
 224 (<5). Some structural fragments of these molecules are evident, such as the case of 9h-fluorene and
 225 Piperazine (Figure 2). Thiazol was common for ZI-187 and ZI-906 (Figure 2A, 2C). Fluorene or 9H-
 226 fluorene is a polycyclic aromatic hydrocarbon insoluble in water and many of its derivatives have
 227 attracted wide attention as basic building blocks for the production of pharmaceuticals, drugs,
 228 lubricating materials, and thermosetting plastics [52]. Piperazine on the other hand, is an organic
 229 compound and heterocyclic amine, this has proven to be of great significance in the rational
 230 development of drugs and its found in well-known drugs with various therapeutic uses, such as
 231 antipsychotic, antihistamine, antianginal, antidepressant, anticancer, antiviral, cardio protectors,
 232 anti-inflammatory, and imaging agents [53]. However, the properties of these fragments alone change
 233 considerably when they are part of other chemical molecules. Finally, the molecule ZI-498 belongs to the library
 234 of natural compounds and presents structural fragments different from the molecules previously described, ZI-
 235 498 include naphthalene, piperidine, and benzene (Figure 2D).

236

237 2.1.3 Molecule - protein interaction and solubility analysis

238

239 The presence of one or two hydrogen bridges was confirmed (Table S7) using the interaction
 240 complexes in the pockets established by the two predictors between the selected molecules and the
 241 3IPK and 3QE5 proteins. This finding could indicate that the interaction between each molecules ZI-
 242 187, ZI-939 and ZI-906 with both proteins, would have very stable couplings, resulting in a possible
 243 inhibition of the *S. mutans* adhesion, since it has been shown that hydrogen bridges regulate and
 244 facilitate molecular interactions [54–58].

245

246

247

248

249

250

251

252

253

254

255

256

257

258

259

260

261

262

263

264

265

266

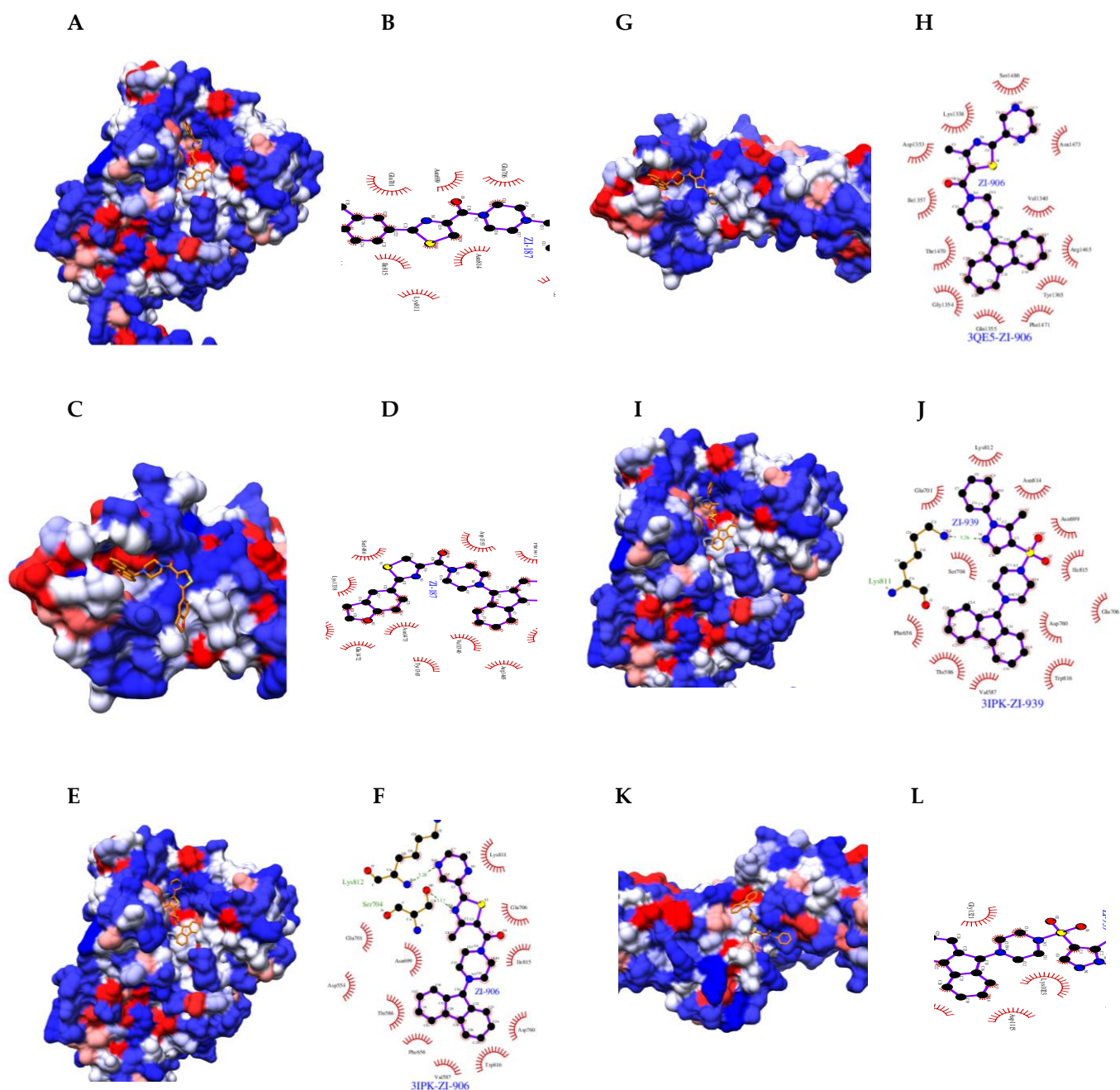
267

268

269

270

271



272 **Figure 3.** Comparison of the interactions of three molecules with A3VP1 region (PDB: 3IPK) and
 273 C-terminal region (PDB: 3QE5) from Ag I/II of *S. mutans*. Hydrophobicity in surface form is shown
 274 for the A3VP1 region interacting with (A) ZI-187, (E) ZI-906 and (I) ZI-939 and C-terminal region
 275 interacting with (C) ZI-187, (G) ZI-906 and (K) ZI-939, where the color scale corresponds to that blue
 276 is very hydrophilic and red is very hydrophobic. Molecular interactions (to 3 Angstrom radius
 277 from the molecules) between residues from A3VP1 region with (B) ZI-187, (F) ZI-906 and (J) ZI-939
 278 and from C-terminal region with (D) ZI-187, (H) ZI-906 and (L) ZI-939.

279

280

281 Additionally, the hydrophobicity analysis of the two Ag I/II domains (PDB: 3IPK and PDB:
 282 3QE5), showed that the three molecules ZI-187, ZI-906 and ZI-939 have a similar interaction with both
 283 domains, in which the interaction site is characterized by one hydrophobic and hydrophilic regions
 284 (figure 3). The 9h-fluorene fragment, which is present in the three molecules, interacts with the same
 285 residues from PDB: 3IPK domain, Thr586 - Val587 - Phe656 - Asp760 - Trp816, which are
 286 hydrophobic, with the exception of Asp760 (Figure 3B, 3F , 3J). However, the interaction of the 9h
 287 fluorene fragment with PDB domain: 3QE5 is similar for the molecule ZI-187 and ZI-906, which
 288 interact with the residues Val1340 - Gly1354 - Gln1355 - Arg1465 - Thr1470 - Phe1471 (Figure 3D, 3H),
 289 most of them hydrophobic. The molecule ZI-939 also shows interaction with different hydrophobic
 290 residues, but different Ile1157 - Tyr1322 - Ala1323 (Figure 3L). On the other hand, the fragments that
 291 are different within the three molecules, interact mostly with hydrophilic residues; we found that for
 292 the PDB: 3IPK domain the molecules interact in the same way with the residues Asn699 - Glu701 -
 293 Ser704 - Ile815, and the interactions with PDB domain: 3QE5 are also characterized by hydrophilic
 294 residues. Only the molecules ZI-187 and ZI-906 showed interactions with common residues, such as
 295 Lys1338 - Asp1353 - Asn1473 - Ser1486 (Figure 3D, 3H), different from those of ZI -939 which were
 296 Lys1023-Gln1024-Leu1113-Gly1321 (Figure 3L).

297 Finally, a descriptive analysis about water solubility of the molecules was conducted using a
 298 consensus from 3 methods resulting in a low aqueous solubility of the molecules , but this parameter
 299 was no used as a selection criteria for molecule selection (Table S8).

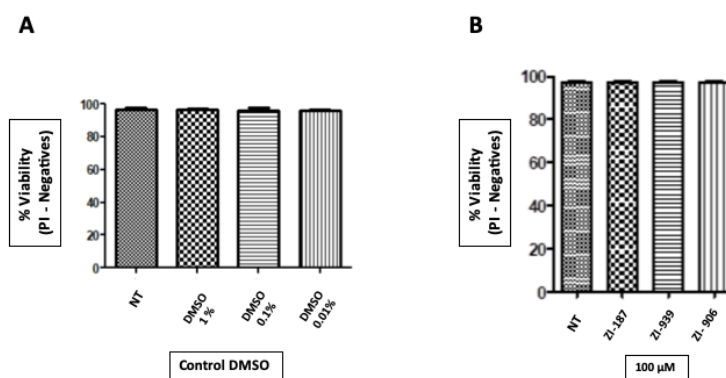
300

301 2.2 *In vitro* assays

302 2.2.1 Cytotoxicity and antimicrobial assays

303 It was found that molecules at concentrations of 100 μ M have no effect on periodontal ligament
 304 fibroblast cells growth and the cells treated with molecules ZI-187 ($P= 0.7372$), ZI-939 ($P= 0.8$) and
 305 ZI-906 ($P= 0.7964$) (Figure 4). However, cells treated with each molecules showed changes in size and
 306 granularity. Therefore, it is important to analyze other human cell lines and add complementary
 307 analysis such as incorporation of DIOC6 for the mitochondrial membrane potential measurement
 308 [59] or apoptosis tests as Annexin V [60]. In addition, for antimicrobial assays molecules at
 309 concentrations of 1000 - 100 - 10 μ M co-cultured experiments with *S. mutans* LT-11 or *C. albicans* -
 310 NCPF 3179, did not affect their growth ($P= <0.001$) (Figure S5 and S6, respectively).

311



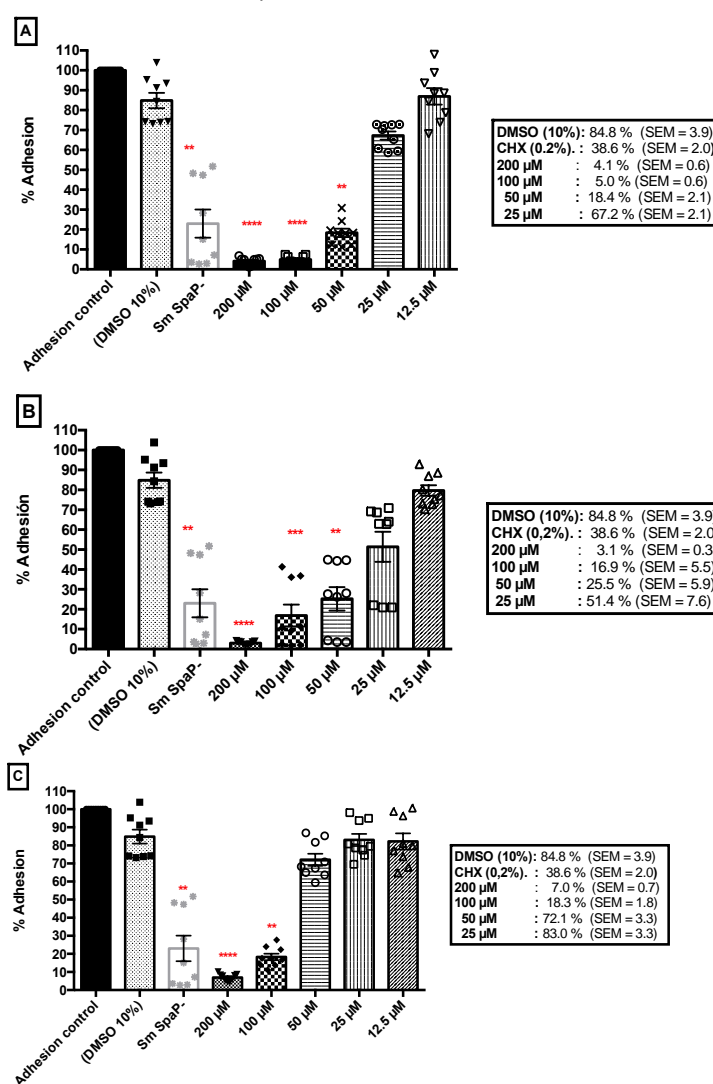
312

313 **Figure 4.** Cytotoxicity evaluation of compounds ZI-187 (P= 0.7372), ZI-939 (P= 0.8) and ZI-906 (P= 0.7964) (100
 314 μM) on periodontal ligament fibroblast cells (PLF), by laminar flow cytometry analysis with Propidium Iodide.
 315

316 2.2.2 Adhesion assays

317 The *S. mutans* LT11 three hours adhesion inhibition test with each molecule selected (ZI-187, ZI-939,
 318 ZI-906) inhibited the surface adhesion to a polystyrene microwell plate. The three molecules showed
 319 an adhesion inhibition greater than 90% at a concentration of 200 μM , 95.9% (SEM = 0.6) with ZI-187,
 320 96.9% (SEM = 0.3) with ZI-906 and 93% (SEM = 0.7) with ZI-939 (Figure 5). This inhibition of adhesion
 321 is maintained above 90% at a concentration of 100 μM only with the molecule ZI-187 (95.0%, SEM =
 322 0.6) (Figure 5A) and for the molecules ZI-906 and ZI-939 the inhibition capacity decreases to 83.1%
 323 (SEM = 5.5) and 81.7% (SEM = 1.8) with ZI-906 and ZI-939 (Figure 5B, 5C), respectively. Interestingly,
 324 the molecules ZI-187 and ZI-906 showed significant differences (P-Value <0,001) in comparison to *S.*
 325 *mutans* Ag I/II deficient (*S. mutans* SpaP-). Up to a concentration of 50 μM , the adhesion inhibition
 326 percentages were 81.6% (SEM = 2.1) for ZI-187 and 74.5% (SEM = 5.9) for ZI-906, but there was no
 327 statistically significant difference for adhesion inhibition of 27.9% (SEM = 3.3) with ZI-939.
 328 Additionally, with these results the IC50 (The half maximal inhibitory concentration) was calculated,
 329 finding that the IC50 for ZI-187 was 27.6 μM (95% CI = 17,4 - 44,5) (Figure 5-A), IC50 of 28.3 μM (95%
 330 IC = 20,2 – 39,8) for ZI-906 and IC50 of 59.5 μM (95% CI = 37,4 - 95,8) for ZI-939.

331



332

333

334 **Figure 5.** Surface adhesion of *S. mutans* - LT11 to a polystyrene microwell plate treated with
 335 molecules (A) ZI-187, (B) ZI-906 and (C) ZI-939. The asterisks represent the level of significance.

336 These findings show the importance of the molecules fragments (9h-fluorene and Piperazine) in
337 the adhesion inhibition, because it has been shown that bacteria have mechanisms that modify the
338 surfaces to increase hydrophobicity and be able to adhere [61,62]. For this study, it was found that
339 the 9h fluorene fragment is very important for adhesion inhibition of *S. mutans*, since the three
340 molecules contain this fragment and interact with hydrophobic parts of the residues and additionally
341 the other fragments such as 2,3 Dihydrobenzofuran in ZI-187, could be important for inhibition
342 capacity.

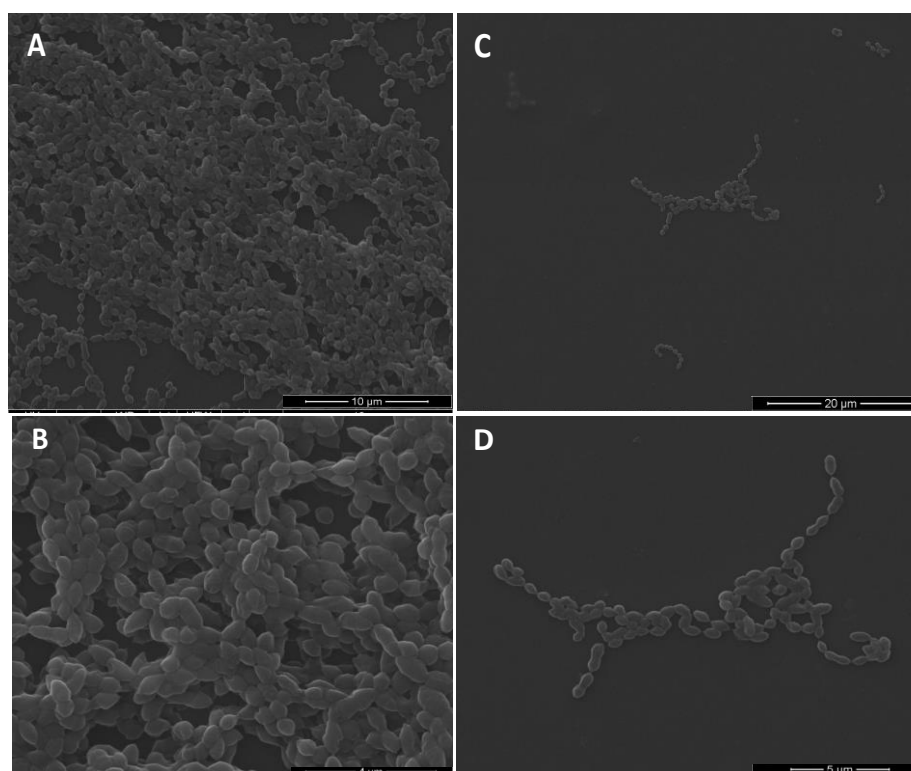
343

344 Additionally, an agglutination phenomenon was observed when molecules with the bacteria
345 was mixed, only at concentrations where the inhibition was affected (Figure S7). ZI-187 was the only
346 molecule that maintained adhesion inhibition above 90% at a concentration of 100 μM , hence this was
347 selected for scanning electron microscopy. Reduction of adherent bacteria was evident, and we did
348 not observe morphological changes in *S. mutans* following treatment with ZI-187, bacteria had intact
349 cell structure and round shapes with smooth edges (Figure 6).

350

351

352



353

354

355 **Figure 6.** Scanning electron microscopy of *S. mutans*-LT11 surface adhesion to a polystyrene
356 microwell plate. Without treatment at 7,000x (A) and 19,000x (B); and treated with 100 μM of
357 molecule ZI-187, at of 4,000x (C) and 11,000x (D).

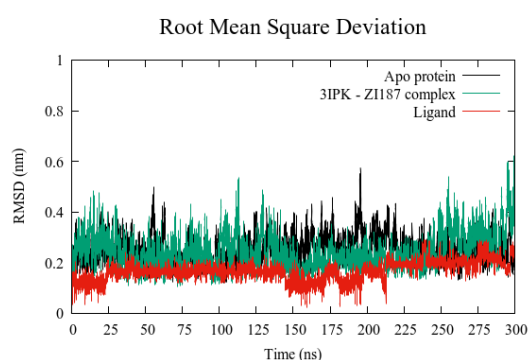
358 There are multiple chemical strategies that could limit the development of dental biofilm,
359 however, most of them can have side effects on teeth, soft tissues or killing oral microbiota, which
360 show the need for specific therapies for cariogenic bacteria. Several studies have focused on blocking
361 two important mechanisms for *S. mutans* biofilm development, such as avoiding sucrose-dependent
362 or sucrose-independent adhesion and interference of cellular signaling “Quorum sensing” [10]. This
363 study was carried out avoiding the sucrose-independent adhesion way, which has been aimed

364 mainly at blocking sortase A, a transpeptidase involved at the anchoring of cell surface proteins,
 365 including Ag I/II, through the LPXTG motif. It has been found that several molecules can reduce
 366 biofilm formation, through the inhibition of the sortase A [63,64], such is the case of the natural phenol
 367 curcumin, (*Curcuma longa*) with which it has been reported inhibition *S. mutans* sortase A activity
 368 with IC50: 10 μ M and a MIC of 175 μ M [65]. However, despite the multiple benefits of this molecule,
 369 some toxic effects have also been evidenced related to the high doses as result from its use as a
 370 supplement in the diet [40,41]. Another natural product is named Morin, it has an inhibitory effect
 371 against *S. mutans* SrtA with IC50: 27.2 μ M [66,67]. Morin other natural product, has an inhibitory
 372 effect against *S. mutans* SrtA with IC50: 27.2 μ M [68], similar to the IC50 obtained with our molecules
 373 ZI-187 and ZI-939 (IC50: 27,6 y 28,3 μ M, respectively). However, the antimicrobial activity of Morin
 374 has also been reported against *S. mutans* [69], differently from the molecules found in this study that
 375 did not present cytotoxic or antimicrobial activities.

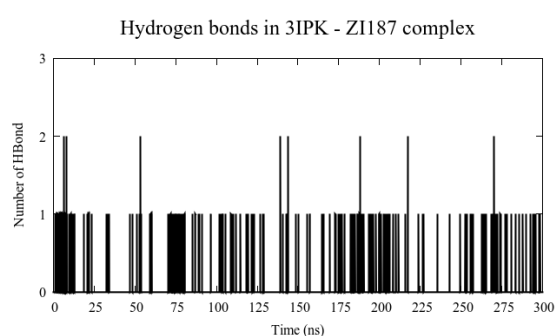
376 2.2.3 Molecular dynamics simulations (MD)

377 Using molecular dynamics simulation, we have found that the complex 3IPK/ZI-187 attained a
 378 high stability after 300ns, during this time the 3IPK protein did not have strong changes when it was
 379 coupled with ZI-187 (Figure 7A), which could indicate that the interacting molecule moves on the
 380 pocket, but not drastically, this means that it does not destabilize the complex; in agreement with the
 381 RMSD result, no significant fluctuation of amino acid residues was observed, however, between
 382 residues 550-600 and 800-850, some differences were showed between the APO protein for 3IPK
 383 (black) and the complex (red) (Figure 7B), which could be due to the specific 3IPK residues that
 384 interact with ZI-187, since different types of interactions of ZI-187 with residues Leu 553 - Asp 554 -
 385 Thr 586 - Val 587 and Lys 811 - Lys 812 - Asn 814 - Ile 815 - Trp 816 were identified (Figure S6). In
 386 addition, 1 and 2 H-bonds were observed between the complex during the simulation time (Figure
 387 7C) and a constant protein structure compactness in the complex (Figure 7D), these two parameters
 388 would support the stability of the interaction between ZI-187 and 3IPK, giving a possible explanation
 389 for the molecule's ability to inhibit the adhesion of *S. mutans*.

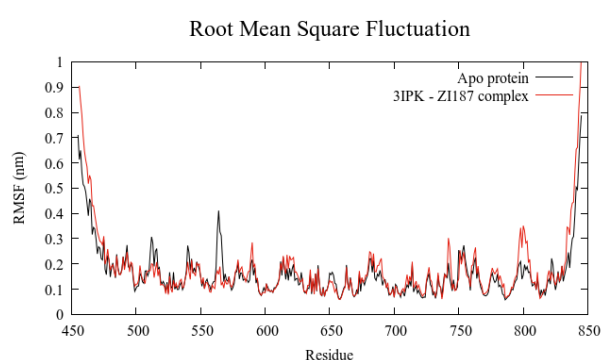
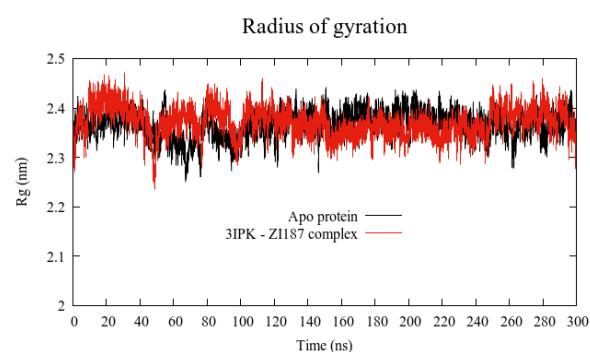
390

391 **A**

392

393 **C**

394

B**D**

395 **Figure 7.** Molecular dynamics simulations analysis. RMSD (Root Mean Square Deviation) (A) -
396 RMSF (Root Mean Square Deviation) (B), hydrogen bonds (C) and Radius of gyration (D) calculated
397 for ZI-187/3IPK complex.

398

399 Finally, the present work allowed to establish a virtual search strategy and selection pipeline for
400 adhesion inhibitory molecules of a cariogenic bacteria but that could be applicable to any pathogen.
401 This study, to the best of our knowledge, is the first report that uses the *S. mutans* Ag I/II as a target,
402 since the previous studies were mainly performed on Gtfs or sortase A proteins. Three molecules
403 were selected ZI-187, ZI-939 and ZI-906, without showing any cytotoxic effect on periodontal
404 ligament fibroblasts or antimicrobial activity on *S. mutans* or *C. albicans*. However, it is suggested to
405 perform assays in other different human cell lines, as well as on other microorganisms of oral cavity
406 importance to evaluate in a much wider range other possible effects. It was also found, as expected,
407 that the molecules selected had a significant effect in terms of reduction of the *S. mutans* surface
408 adhesion as a single microorganism, but it is very important to carry out complementary studies on
409 multispecies biofilms models, also to identify through transcriptomic analysis if there are variations
410 on the expression of adhesion genes dependent and independent of sucrose when treating bacteria
411 with the selected molecules, as well as genes that participate in cell signaling during the biofilm
412 development process. Similarly, an *in vivo* cariogenic model should be established in order to insight
413 the anti-cariogenic capacity of these molecules.

414 3. Materials and Methods

415 3.1 Structure based virtual Screening

416 3.1.1 Target proteins selection

417 3D protein structures for the virtual search were selected using the Ag I/II of *S. mutans* sequence
418 AFR75221.1 (NCBI <https://www.ncbi.nlm.nih.gov/>) and the 3D SWISS-MODEL software
419 (<http://swissmodel.expasy.org/>). 3D structures of two Ag I/II protein fragments 3IPK (PDB-ID) [21]
420 and 3QE5 [20], were used for a sequence and protein structure similarity analysis using a BLAST-P
421 (Protein Basic Local Alignment Search Tool - NCBI) and the FAT-CAT server (Flexible structure
422 Alignment by Chaining Aligned fragment pairs allowing Twists) [70] to search for similar (rigid)
423 protein structures, using similarities only with a P-value <0.05. Subsequently, for 3IPK and 3QE5
424 proteins an analysis of binding sites "Pockets" using meta-servers MetaPocket 2.0 [49] and COACH
425 [50] was carried out. 3D structures of the proteins were obtained in PDB format and edited in
426 AutoDockTools 4.0 (<http://mgltools.scripps.edu>) [71]. Molecular docking of molecules with AgI/II
427 protein fragments, was performed at the Texas Advanced Computing Center (TACC: Texas
428 Advanced Computing Center; Austin, TX) using 3 libraries "ZINC (Lrg)" of ~ 642,759, Library "ZINC
429 (Sm)" of ~ 46,702 molecules, and "ZINC Natural Cmpds (Large)" of 194,090 from the ZINC15 database
430 [72], a total of ~ 883,551 molecules.

431 3.1.2 Molecules selection:

432 Two methodologies were used for molecules selection, one according to the molecular docking
433 score and other according to the number of pockets in which molecules interacted, classification of
434 molecules that interacted in most pockets was carried out using a script executed in the R-studio
435 package (Version 1.0.156); ten molecules were arbitrarily selected from each methodology. An *in silico*
436 analysis was performed using the QuikProp application (Version 3.2) from Schrödinger software [73],
437 according to [74] with some modifications, in order to analyze pharmacokinetic profiles such as
438 absorption, distribution, metabolism and excretion (ADME). Molecules that had more than two
439 violations of the Lipinski's Rules and that did not comply with more than two of the standard

440 physical-chemical parameters established by 95% of the known drugs, according to Schrödinger's
441 QuikProp program repositories, were excluded.

442 For computational toxicity prediction of the molecules, the Protox-II program was used [75], for
443 acute toxicity, hepatotoxicity, cytotoxicity, carcinogenicity, mutagenicity and immunotoxicity. In
444 addition, the molecules lethal dose 50 (LD50) (mg/kg) was calculated and classified according to the
445 Globally Harmonized System of Classification and Labeling of Chemicals (GHS). For this analysis,
446 chlorhexidine was used as the reference drug, one of the most commonly prescribed antiseptic agents
447 in dentistry; the experimental LD50 values of oral administration in mice of this drug were taken
448 from the Pfizer chlorhexidine technical data sheet [76]. Molecules above class 3 and without any
449 probability of toxicity were selected.

450 3.1.3 Molecule - protein interaction and solubility analysis

451 ZINC19835187 (Database code Zinc15), ZINC19924906 and ZINC19924939, (ZI-187, ZI-906 and
452 ZI-939, respectively) were selected and the H-bonding and hydrophobicity interactions between the
453 molecules and the two protein fragments 3ipk - 3qe5 were identified [77] using Biovia Discovery
454 Studio [78] and Chimera [79] softwares. The swissADME web server (<http://www.swissadme.ch/>)
455 was used to predict water solubility characteristics of the molecules, using a consensus of three
456 methods Log S (ESOL), Log S (Ali) and Log S (SILICOS- IT) [80].

457 3.2 In vitro assays

458 Three molecules were purchased (ZI-498 was not available for sale) from the MolPort company
459 (<https://www.molport.com>). Stock solution of the molecules were diluted in 100% DMSO (dimethyl
460 sulfoxide) at a concentration of 10^4 μ M (ZI-187 (MW = 479.6) = 4796 μ g/ml; ZI-906 (MW = 453.6) =
461 4535,6 μ g/ml; ZI-939 (MW = 470.6) = 4075,9 μ g/ml).

462 3.2.1 Cytotoxicity and antimicrobial assays:

463 Cytotoxic effects of ZI-187, ZI-906 and ZI-939 on periodontal ligament fibroblast cells (FLP)
464 treated for 24 hours with each molecule was evaluated and analyzed by flow cytometry with
465 propidium iodide (PI), using 100 μ M of each molecules and DMSO 1%. *S. mutans* - Lt11 (UB579 WT)
466 [81] and *C. albicans* NCPF 3179 (NCPF, 1986) were cultured overnight in broth BHI BD® at 37 °C
467 shaking at 250 RPM. The next day, *S. mutans* and *C. albicans* suspension in BHI broth (180 μ l/well,
468 OD_{600nm} = 0.1) was seeded into 96-well plates (Costar, Cambridge, MA) with 20 μ l of the molecules
469 (concentrations of 1.000, 100, 10, μ M. DMSO 10%), as a negative control (death) 0.2% Chlorhexidine
470 digluconate (Farpag®) was used, while the corresponding broth without molecules were used as a
471 positive growth control, as well as those treated with DMSO 10% [82]. After incubation for 24 hours
472 at 37°C shaking at 250 RPM, the absorbance was measured in an Epoch™ Microplate
473 spectrophotometer (BioTek®) (OD_{600nm}), to evaluate cell growth and to establish the minimum
474 inhibitory concentration (MIC)

475 3.2.2 Adhesion assay:

476 *S. mutans*-Lt11 (UB579 WT) was cultured in BHI broth (BD®) overnight at 37 °C shaking at 250
477 RPM. The culture medium was discarded and bacteria were washed with phosphate buffer solution
478 (PBS 1X) by centrifugation at 3000 RPM for 10 minutes. Subsequently, bacterial suspension in PBS
479 1X, OD_{600nm} = 1 was measured using an Epoch™ Microplate spectrophotometer (BioTek®) and 180 μ l
480 were inoculated into a 96-well microplate (NEST®, Ref: 701001) with 20 μ l of each molecule at 200,
481 100, 50, 25, 12.5 μ M and incubated for three hours at 37 °C shaking at 250 RPM [83]. *S. mutans* SpaP-
482 strain (mutant for AgI/II also called SpaP) and *S. mutans*-Lt11 treated with DMSO 10% were used as
483 control. Plate wells were washed with water and adherent cells were stained by adding 200 μ L 0.05%

484 crystal violet for 15 min, washed and measured by absorbance at 600 nm after addition of 30% glacial
485 acetic acid.

486 3.2.3 Data analysis

487 All experiments were performed in triplicate and reproduced three separate times. Cell viability
488 percentages were reported as negative % PI \pm SEM and analyzed by one-way ANOVA, followed by
489 a Dunnett's multiple comparison test. In *S. mutans* and *C. albicans* growth and adhesion inhibition
490 analysis, the OD data were normalized to percentages and analyzed using D'Agostino & Pearson
491 omnibus and Shapiro-Wilk normality test; subsequently the nonparametric Kruskal–Wallis test with
492 Dunnett's multiple comparisons against the controls *S. mutans* and *C. albicans* treated with DMSO
493 10%. Finally, the half maximal inhibitory concentration (IC50) was calculated. GraphPad Prism
494 version 6.0 (GraphPad Software, La Jolla California USA, www.graphpad.com) was used and values
495 of $P < 0.05$ were considered statistically significant.

496 3.2.4 Scanning Electron Microscopy (SEM):

497 Surface adhesion assays were performed on Thermo Scientific Nunc Lab-Tek and Lab Tek II Chamber
498 Slides, using *S. mutans* - Lt11 untreated and treated with molecule ZI-187 (100 μ M). After incubation
499 for three hours at 37 °C shaking at 250 RPM, each sample was washed three times with PBS 1X, then
500 the samples were fixed with 2,5% glutaraldehyde (0.1M PBS) for 24 hours at 4 °C. Finally, the slides
501 were washed three times with distilled water and dehydrated by immersion in solutions of ascending
502 concentrations of ethanol 70, 90 and 100% (10 minutes each) and dried overnight in a laminar flow
503 cabinet. The samples were covered with gold and visualized using a FEI QUANTA-200TM scanning
504 electron microscope with a variable range acceleration voltage of 1–30 KV.

505 3.2.5 Molecular dynamics simulations (MD)

506 MD simulations were carried out using the GROMACS 4.5.5 package [84]. Molecule ZI-187 was
507 docked to the 3IPK protein pocket with the highest binding affinity (P1 by COACH predictor). The
508 ZI-187/3IPK complex and the 3IPK protein in its APO state (reference state), were used as initial
509 coordinates for MD simulations. Finally, both systems were subjected to a 300ns production stage,
510 using a 2fs time step. The equilibrations and productions were carried out using a temperature of
511 310K (36.85 °C) and a 1 bar pressure. Descriptors such as the RMSD (Root of the mean square
512 deviation), the RMSF (Root of the mean square fluctuation) and hydrogen bonds present in the
513 protein-ligand complex were followed with the tools contained *g_rms*, *g_rmsf* and *g_hbond*,
514 respectively.

515

516 Author Contributions:

517 “Conceptualization, Raul E. Rivera, Nestor I. Cardona and Leonardo Padilla; methodology, Raul E. Rivera,
518 Mayri A. Diaz De Rienzo, Wbeimar Rivera, Sandra M. Morales and Maria C. Martinez; software, Raul E. Rivera,
519 Cristian C. Rocha; validation, Raul E. Rivera, Cristian C. Rocha, Nestor I. Cardona and Leonardo Padilla; formal
520 analysis, Raul E. Rivera, Mayri A. Diaz De Rienzo, Wbeimar Rivera, Sandra M. Morales and Maria C. Martinez;
521 investigation, X.X.; resources, X.X.; data curation, Raul E. Rivera, Cristian C. Rocha, Wbeimar Rivera; writing—
522 original draft preparation, Raul E. Rivera.; writing—review and editing, Raul E. Rivera, Nestor I. Cardona,
523 Wbeimar Rivera, Cristian C. Rocha, Mayri A. Diaz De Rienzo, Sandra M. Morales, Maria C. Martinez. authors
524 have read and agreed to the published version of the manuscript.”

525

526 **Funding:** “This research was funded by COLCIENCIAS, grant number 727-2015 ”

527 **Acknowledgments:** The authors acknowledge the assistance of Mr Paul Gibbons (Liverpool John Moores
528 University), with the SEM experiments; the *S. mutans* strain donation by Dr. Jane Brittan from the Oral

529 Microbiology Laboratory, Bristol School of Dentistry, University of Bristol (UK), Bristol; the script design by Dr.
530 Gladys Elena Salcedo Echeverry and Dr. Aylan Farid Arenas from Research Group and Counseling in Statistics
531 of the University of Quindío.

532

533 **Conflicts of Interest:** “The authors declare no conflict of interest

534 References

- 535 1. Kyu, H.H.; Abate, D.; Abate, K.H.; Abay, S.M.; Abbafati, C.; Abbasi, N.; Abbastabar, H.; Abd-Allah, F.;
536 Abdela, J.; Abdelalim, A.; et al. glo. *Lancet* **2018**, doi:10.1016/S0140-6736(18)32335-3.
- 537 2. Vos, T.; Allen, C.; Arora, M.; Barber, R.M.; Brown, A.; Carter, A.; Casey, D.C.; Charlson, F.J.; Chen, A.Z.;
538 Coggeshall, M.; et al. Global, regional, and national incidence, prevalence, and years lived with disability
539 for 310 diseases and injuries, 1990–2015: a systematic analysis for the Global Burden of Disease Study
540 2015. *Lancet* **2016**, doi:10.1016/S0140-6736(16)31678-6.
- 541 3. Lu, M.; Xuan, S.; Wang, Z. Oral microbiota: A new view of body health. *Food Sci. Hum. Wellness* **2019**, *8*,
542 8–15, doi:10.1016/j.fshw.2018.12.001.
- 543 4. Tanzer, J.M. Dental Caries is a Transmissible Infectious Disease: The Keyes and Fitzgerald Revolution.
544 *J. Dent. Res.* **1995**, *74*, 1536–1542, doi:10.1177/00220345950740090601.
- 545 5. Selwitz, R.H.; Ismail, A.I.; Pitts, N.B. Dental caries. *Lancet* **2007**, *369*, 51–59,
546 doi:http://dx.doi.org/10.1016/S0140-6736(07)60031-2.
- 547 6. Kolenbrander, P.E.; Palmer, R.J.; Periasamy, S.; Jakubovics, N.S. Oral multispecies biofilm development
548 and the key role of cell-cell distance. *Nat. Rev. Microbiol.* **2010**, *8*, 471–480, doi:10.1038/nrmicro2381.
- 549 7. Moschioni, M.; Pansegrau, W.; Barocchi, M.A. Adhesion determinants of the Streptococcus species.
550 *Microb. Biotechnol.* **2010**, *3*, 370–388, doi:10.1111/j.1751-7915.2009.00138.x.
- 551 8. Matsumoto-Nakano, M. Role of Streptococcus mutans surface proteins for biofilm formation. *Jpn. Dent.*
552 *Sci. Rev.* **2018**, *54*, 22–29, doi:10.1016/j.jdsr.2017.08.002.
- 553 9. Krzyściak, W.; Jurczak, A.; Kościelniak, D.; Bystrowska, B.; Skalniak, A. The virulence of Streptococcus
554 mutans and the ability to form biofilms. *Eur. J. Clin. Microbiol. Infect. Dis.* **2014**, *33*, 499–515,
555 doi:10.1007/s10096-013-1993-7.
- 556 10. Scharnow, A.M.; Solinski, A.E.; Wuest, W.M. Targeting: S. mutans biofilms: A perspective on preventing
557 dental caries. *Medchemcomm* **2019**, *10*, 1057–1067, doi:10.1039/c9md00015a.
- 558 11. Mitchell, T.J. The pathogenesis of streptococcal infections: from Tooth decay to meningitis. *Nat. Rev.*
559 *Microbiol.* **2003**, *1*, 219–230, doi:10.1038/nrmicro771.
- 560 12. Lamont, R.J.; Demuth, D.R.; Davis, C.A.; Malamud, D.; Rosan, B. Salivary-agglutinin-mediated
561 adherence of Streptococcus mutans to early plaque bacteria. *Infect. Immun.* **1991**, *59*, 3446–3450,
562 doi:10.1128/iai.59.10.3446-3450.1991.

- 563 13. Jakubovics, N.S.; Strömberg, N.; Van Dolleweerd, C.J.; Kelly, C.G.; Jenkinson, H.F. Differential binding
564 specificities of oral streptococcal antigen I/II family adhesins for human or bacterial ligands. *Mol.*
565 *Microbiol.* **2005**, *55*, 1591–1605, doi:10.1111/j.1365-2958.2005.04495.x.
- 566 14. Pecharki, D.; Petersen, F.C.; Assev, S.; Scheie, A.A. Involvement of antigen I/II surface proteins in
567 *Streptococcus mutans* and *Streptococcus intermedius* biofilm formation. *Oral Microbiol. Immunol.* **2005**,
568 *20*, 366–371, doi:10.1111/j.1399-302X.2005.00244.x.
- 569 15. Crowley, P.J.; Brady, L.J.; Michalek, S.M.; Bleiweis, A.S. Virulence of a spaP mutant of *Streptococcus*
570 *mutans* in a gnotobiotic rat model. *Infect. Immun.* **1999**, *67*, 1201–1206, doi:10.1128/iai.67.3.1201-1206.1999.
- 571 16. Matsushita, K.; Nisizawa, T.; Nagaoka, S.; Kawagoe, M.; Koga, T. Identification of antigenic epitopes in
572 a surface protein antigen of *Streptococcus mutans* in humans. *Infect. Immun.* **1994**, *62*, 4034–4042,
573 doi:10.1128/iai.62.9.4034-4042.1994.
- 574 17. Robinette, R.A.; Heim, K.P.; Oli, M.W.; Crowley, P.J.; McArthur, W.P.; Brady, L.J. Alterations in
575 immunodominance of *Streptococcus mutans* AgI/II: Lessons learned from immunomodulatory
576 antibodies. *Vaccine* **2014**, *32*, 375–382, doi:10.1016/j.vaccine.2013.11.023.
- 577 18. Batista, M.T.; Souza, R.D.; Ferreira, E.L.; Robinette, R.; Crowley, P.J.; Rodrigues, J.F.; Jeannine Brady, L.;
578 Ferreira, L.C.S.; Ferreira, R.C.C. Immunogenicity and in vitro and in vivo protective effects of antibodies
579 targeting a recombinant form of the *Streptococcus mutans* P1 surface protein. *Infect. Immun.* **2014**, *82*,
580 4978–4988, doi:10.1128/IAI.02074-14.
- 581 19. Jenkinson, H.F.; Demuth, D.R. Structure, function and immunogenicity of streptococcal antigen I/II
582 polypeptides. *Mol. Microbiol.* **1997**, *23*, 183–190, doi:10.1046/j.1365-2958.1997.2021577.x.
- 583 20. Larson, M.R.; Rajashankar, K.R.; Crowley, P.J.; Kelly, C.; Mitchell, T.J.; Brady, L.J.; Deivanayagam, C.
584 Crystal structure of the C-terminal region of *Streptococcus mutans* antigen I/II and characterization of
585 salivary agglutinin adherence domains. *J. Biol. Chem.* **2011**, *286*, 21657–21666,
586 doi:10.1074/jbc.M111.231100.
- 587 21. Larson, M.R.; Rajashankar, K.R.; Patel, M.H.; Robinette, R.A.; Crowley, P.J.; Michalek, S.; Brady, L.J.;
588 Deivanayagam, C. Elongated fibrillar structure of a streptococcal adhesin assembled by the high-affinity
589 association of alpha- and PPII-helices. *Proc. Natl. Acad. Sci. U. S. A.* **2010**, *107*, 5983–8,
590 doi:10.1073/pnas.0912293107.
- 591 22. Brady, L.J.; Maddocks, S.E.; Larson, M.R.; Forsgren, N.; Persson, K.; Deivanayagam, C.C.; Jenkinson,
592 H.F. The changing faces of *Streptococcus* antigen I/II polypeptide family adhesins: MicroReview. *Mol.*
593 *Microbiol.* **2010**, *77*, 276–286, doi:10.1111/j.1365-2958.2010.07212.x.
- 594 23. Yang, C.; Scoffield, J.; Wu, R.; Deivanayagam, C.; Zou, J.; Wu, H. Antigen I/II mediates interactions
595 between *Streptococcus mutans* and *Candida albicans*. *Mol. Oral Microbiol.* **2018**, *176*, 139–148,
596 doi:10.1111/omi.12223.Antigen.
- 597 24. Yang, J.; Deng, D.; Brandt, B.W.; Nazmi, K.; Wu, Y.; Crielaard, W.; Ligtenberg, A.J.M. Diversity of SpaP

- 598 in genetic and salivary agglutinin mediated adherence among *Streptococcus mutans* strains. *Sci. Rep.*
599 **2019**, *9*, 1–9, doi:10.1038/s41598-019-56486-9.
- 600 25. Esberg, A.; Löfgren-Burström, A.; Öhman, U.; Strömberg, N. Host and bacterial phenotype variation in
601 adhesion of *Streptococcus mutans* to matched human hosts. *Infect. Immun.* **2012**, *80*, 3869–3879,
602 doi:10.1128/IAI.00435-12.
- 603 26. Janakiram, C.; Deepan Kumar, C. V.; Joseph, J. Xylitol in preventing dental caries: A systematic review
604 and meta-analyses. *J. Nat. Sci. Biol. Med.* **2017**, *8*, 16–21, doi:10.4103/0976-9668.198344.
- 605 27. Riley, P.; Moore, D.; Ahmed, F.; Sharif, M.O.; Worthington, H. V. Xylitol-containing products for
606 preventing dental caries in children and adults. *Cochrane database Syst. Rev.* **2015**, *3*, CD010743,
607 doi:10.1002/14651858.CD010743.pub2.
- 608 28. Autio-Gold, J. The role of chlorhexidine in caries prevention. *Oper. Dent.* **2008**, *33*, 710–716,
609 doi:10.2341/08-3.
- 610 29. Walsh, T.; Oliveira-Neto, J.M.; Moore, D. Chlorhexidine treatment for the prevention of dental caries in
611 children and adolescents. *Cochrane Database Syst. Rev.* **2015**, *2015*, doi:10.1002/14651858.CD008457.pub2.
- 612 30. Koga, T.; Oho, T.; Shimazaki, Y.; Nakano, Y. Immunization against dental caries. *Vaccine* **2002**, *20*, 2027–
613 2044, doi:10.1016/S0264-410X(02)00047-6.
- 614 31. Oh, D.H.; Chen, X.; Daliri, E.B.M.; Kim, N.; Kim, J.R.; Yoo, D. Microbial etiology and prevention of dental
615 caries: Exploiting natural products to inhibit cariogenic biofilms. *Pathogens* **2020**, *9*, 1–15,
616 doi:10.3390/pathogens9070569.
- 617 32. Ren, Z.; Chen, L.; Li, J.; Li, Y. Inhibition of *Streptococcus mutans* polysaccharide synthesis by molecules
618 targeting glycosyltransferase activity. **2016**, *1*.
- 619 33. Tada, A.; Nakayama-Imahiji, H.; Yamasaki, H.; Hasibul, K.; Yoneda, S.; Uchida, K.; Nariya, H.; Suzuki,
620 M.; Miyake, M.; Kuwahara, T. Cleansing effect of acidic L-arginine on human oral biofilm. *BMC Oral*
621 *Health* **2016**, *16*, 1–9, doi:10.1186/s12903-016-0194-z.
- 622 34. Madrid Troconis, C.C.; Perez Puello, S.D.C. Nanocomplejo De Fosfopéptido De Caseína-Fosfato De
623 Calcio Amorfo (Cpp-Acp) En Odontología: Estado Del Arte. *Rev. Fac. Odontol.* **2019**, *30*, 248–263,
624 doi:10.17533/udea.rfo.v30n2a10.
- 625 35. Bijle, M.N.A.; Ekambaram, M.; Lo, E.C.M.; Yiu, C.K.Y. The combined antimicrobial effect of arginine and
626 fluoride toothpaste. *Sci. Rep.* **2019**, *9*, 1–10, doi:10.1038/s41598-019-44612-6.
- 627 36. Zheng, X.; He, J.; Wang, L.; Zhou, S.; Peng, X.; Huang, S.; Zheng, L.; Cheng, L.; Hao, Y.; Li, J.; et al.
628 Ecological Effect of Arginine on Oral Microbiota. *Sci. Rep.* **2017**, *7*, 1–10, doi:10.1038/s41598-017-07042-w.
- 629 37. Ferrer, M.D.; López-López, A.; Nicolescu, T.; Perez-Vilaplana, S.; Boix-Amorós, A.; Dzidic, M.; Garcia,
630 S.; Artacho, A.; Llana, C.; Mira, A. Topic Application of the Probiotic *Streptococcus dentisani* Improves
631 Clinical and Microbiological Parameters Associated With Oral Health. *Front. Cell. Infect. Microbiol.* **2020**,

- 632 10, 1–14, doi:10.3389/fcimb.2020.00465.
- 633 38. Mayr, L.M.; Fuerst, P. The Future of High-Throughput Screening. *J. Biomol. Screen.* **2008**, *13*, 443–448,
634 doi:10.1177/1087057108319644.
- 635 39. Mohs, R.C.; Greig, N.H. Drug discovery and development: Role of basic biological research. *Alzheimer's*
636 *Dement. Transl. Res. Clin. Interv.* **2017**, *3*, 651–657, doi:10.1016/j.trci.2017.10.005.
- 637 40. Sinha, S.; Vohora, D. *Drug Discovery and Development: An Overview*; Elsevier Inc., 2017; ISBN
638 9780128021033.
- 639 41. Barbosa, A.; Romário, D.; Avelar, S.; Gomes, G.; Albuquerque, A.R.; Gaudencio, T. In Silico Approach
640 for the Identification of Potential Targets and Specific Antimicrobials for *Streptococcus mutans*. *Adv*
641 *Biosci Biotech* **2014**, *5*, 373–385.
- 642 42. Ren, Z.; Cui, T.; Zeng, J.; Chen, L.; Zhang, W.; Xu, X.; Cheng, L.; Li, M.; Li, J.; Zhou, X.; et al. Molecule
643 targeting glucosyltransferase inhibits *Streptococcus mutans* biofilm formation and virulence. *Antimicrob.*
644 *Agents Chemother.* **2016**, *60*, 126–135, doi:10.1128/AAC.00919-15.
- 645 43. Zhang, Q.; Nijampatnam, B.; Hua, Z.; Nguyen, T.; Zou, J.; Cai, X.; Michalek, S.M.; Velu, S.E.; Wu, H.
646 Structure-Based Discovery of Small Molecule Inhibitors of Cariogenic Virulence. *Sci. Rep.* **2017**, *7*, 1–10,
647 doi:10.1038/s41598-017-06168-1.
- 648 44. Troffer-Charlier, N.; Ogier, J.; Moras, D.; Cavarelli, J. Crystal structure of the V-region of streptococcus
649 *mutans* antigen I/II at 2.4 Å resolution suggests a sugar preformed binding site. *J. Mol. Biol.* **2002**, *318*,
650 179–188, doi:10.1016/S0022-2836(02)00025-6.
- 651 45. Nylander, Å.; Forsgren, N.; Persson, K. Structure of the C-terminal domain of the surface antigen SpaP
652 from the caries pathogen *Streptococcus mutans*. *Acta Crystallogr. Sect. F Struct. Biol. Cryst. Commun.* **2011**,
653 *67*, 23–26, doi:10.1107/S174430911004443X.
- 654 46. Heim, K.P.; Crowley, P.J.; Long, J.R.; Kailasan, S.; McKenna, R.; Brady, L.J. An intramolecular lock
655 facilitates folding and stabilizes the tertiary structure of streptococcus *mutans* adhesin p1. *Proc. Natl.*
656 *Acad. Sci. U. S. A.* **2014**, *111*, 15711–15716, doi:10.1073/pnas.1413018111.
- 657 47. Lionta, E.; Spyrou, G.; Vassilatis, D.K.; Cournia, Z. Send Orders for Reprints to
658 reprints@benthamscience.net Structure-Based Virtual Screening for Drug Discovery: Principles,
659 Applications and Recent Advances. *Curr. Top. Med. Chem.* **2014**, *14*, 1923–1938,
660 doi:10.2174/1568026614666140929124445.
- 661 48. Gazgalis, D.; Zaka, M.; Zaka, M.; Abbasi, B.H.; Logothetis, D.E.; Mezei, M.; Cui, M. Protein Binding
662 Pocket Optimization for Virtual High-Throughput Screening (vHTS) Drug Discovery. *ACS Omega* **2020**,
663 *5*, 14297–14307, doi:10.1021/acsomega.0c00522.
- 664 49. Huang, B. MetaPocket: A Meta Approach to Improve Protein Ligand Binding Site Prediction. *Omi. A J.*
665 *Integr. Biol.* **2009**, *13*, 325–330, doi:10.1089/omi.2009.0045.

- 666 50. Yang, J.; Roy, A.; Zhang, Y. Protein-ligand binding site recognition using complementary binding-
667 specific substructure comparison and sequence profile alignment. *Bioinformatics* **2013**, *29*, 2588–2595,
668 doi:10.1093/bioinformatics/btt447.
- 669 51. Jenkinson, H.F.; Demuth, D.R. Structure, function and immunogenicity of streptococcal antigen I/II
670 polypeptides. *Mol. Microbiol.* **1997**, *23*, 183–90, doi:10.1046/j.1365-2958.1997.2021577.x.
- 671 52. El-Sayed, R.; Althagafi, I.I.; Ahmed, S.A. Fluorene Derivatives with Multi-addressable Properties:
672 Synthesis, Characterization, and Reactivity. *J. Surfactants Deterg.* **2017**, *20*, 933–945, doi:10.1007/s11743-
673 017-1958-4.
- 674 53. Rathi, A.K.; Syed, R.; Shin, H.S.; Patel, R. V. Piperazine derivatives for therapeutic use: A patent review
675 (2010-present). *Expert Opin. Ther. Pat.* **2016**, *26*, 777–797, doi:10.1080/13543776.2016.1189902.
- 676 54. Hadži, D.; Kidrič, J.; Koller, J.; Mavri, J. The role of hydrogen bonding in drug-receptor interactions. *J.*
677 *Mol. Struct.* **1990**, *237*, 139–150, doi:10.1016/0022-2860(90)80136-8.
- 678 55. Kuhn, B.; Mohr, P.; Stahl, M. Intramolecular hydrogen bonding in medicinal chemistry. *J. Med. Chem.*
679 **2010**, *53*, 2601–2611, doi:10.1021/jm100087s.
- 680 56. Caron, G.; Kihlberg, J.; Ermondi, G. Intramolecular hydrogen bonding: An opportunity for improved
681 design in medicinal chemistry. *Med. Res. Rev.* **2019**, *39*, 1707–1729, doi:10.1002/med.21562.
- 682 57. J. R. Yunta, M. It Is Important to Compute Intramolecular Hydrogen Bonding in Drug Design? *Am. J.*
683 *Model. Optim.* **2017**, *5*, 24–57, doi:10.12691/ajmo-5-1-3.
- 684 58. Ermondi, G.; Caron, G. Why we need to implement intramolecular hydrogen-bonding considerations in
685 drug discovery. *Future Med. Chem.* **2016**, *31*, 48–49.
- 686 59. Cottet-Rousselle, C.; Ronot, X.; Leverve, X.; Mayol, J.F. Cytometric assessment of mitochondria using
687 fluorescent probes. *Cytom. Part A* **2011**, *79 A*, 405–425, doi:10.1002/cyto.a.21061.
- 688 60. Rieger, A.M.; Nelson, K.L.; Konowalchuk, J.D.; Barreda, D.R. Modified annexin V/propidium iodide
689 apoptosis assay for accurate assessment of cell death. *J. Vis. Exp.* **2011**, 3–6, doi:10.3791/2597.
- 690 61. Grivet, M.; Morrier, J.J.; Benay, G.; Barsotti, O. Effect of hydrophobicity on in vitro streptococcal adhesion
691 to dental alloys. *J. Mater. Sci. Mater. Med.* **2000**, *11*, 637–642, doi:10.1023/A:1008913915399.
- 692 62. Wang, C.; van der Mei, H.C.; Busscher, H.J.; Ren, Y. Streptococcus mutans adhesion force sensing in
693 multi-species oral biofilms. *npj Biofilms Microbiomes* **2020**, *6*, 1–9, doi:10.1038/s41522-020-0135-0.
- 694 63. Wang, J.; Shi, Y.; Jing, S.; Dong, H.; Wang, D.; Wang, T. Astilbin Inhibits the Activity of Sortase A from
695 Streptococcus mutans. *Molecules* **2019**, *24*, 465, doi:10.3390/molecules24030465.
- 696 64. Luo, H.; Liang, D.F.; Bao, M.Y.; Sun, R.; Li, Y.Y.; Li, J.Z.; Wang, X.; Lu, K.M.; Bao, J.K. In silico
697 identification of potential inhibitors targeting Streptococcus mutans sortase A. *Int. J. Oral Sci.* **2017**, *9*,
698 53–62, doi:10.1038/ijos.2016.58.

- 699 65. Hu, P.; Huang, P.; Chen, M.W. Curcumin reduces *Streptococcus mutans* biofilm formation by inhibiting
700 sortase A activity. *Arch. Oral Biol.* **2013**, *58*, 1343–1348, doi:10.1016/j.archoralbio.2013.05.004.
- 701 66. Burgos-Morón, E.; Calderón-Montaña, J.M.; Salvador, J.; Robles, A.; López-Lázaro, M. The dark side of
702 curcumin Estefani´a. *Int. J. Cancer* **2010**, *126*, 1771–1775, doi:10.1038/s41567-018-0261-2.
- 703 67. Cianfruglia, L.; Minnelli, C.; Laudadio, E.; Scirè, A.; Armeni, T. Side effects of curcumin: Epigenetic and
704 antiproliferative implications for normal dermal fibroblast and breast cancer cells. *Antioxidants* **2019**, *8*,
705 1–13, doi:10.3390/antiox8090382.
- 706 68. Huang, P.; Hu, P.; Zhou, S.Y.; Li, Q.; Chen, W.M. Morin inhibits sortase A and subsequent biofilm
707 formation in *Streptococcus mutans*. *Curr. Microbiol.* **2014**, *68*, 47–52, doi:10.1007/s00284-013-0439-x.
- 708 69. Yang, J.Y.; Lee, H.S. Evaluation of antioxidant and antibacterial activities of morin isolated from
709 mulberry fruits (*Morus alba* L.). *J. Korean Soc. Appl. Biol. Chem.* **2012**, *55*, 485–489, doi:10.1007/s13765-012-
710 2110-9.
- 711 70. Ye, Y.; Godzik, A. FATCAT: A web server for flexible structure comparison and structure similarity
712 searching. *Nucleic Acids Res.* **2004**, *32*, 582–585, doi:10.1093/nar/gkh430.
- 713 71. Morris, G.M.; Huey, R.; Lindstrom, W.; Sanner, M.F.; Belew, R.K.; Goodsell, D.S.; Olson, A.J. AutoDock4
714 and AutoDockTools4: Automated docking with selective receptor flexibility. *J. Comput. Chem.* **2009**, *30*,
715 2785–91, doi:10.1002/jcc.21256.
- 716 72. Sterling, T.; Irwin, J.J. ZINC 15 - Ligand Discovery for Everyone. *J. Chem. Inf. Model.* **2015**, *55*, 2324–2337,
717 doi:10.1021/acs.jcim.5b00559.
- 718 73. Schrödinger Schrödinger Release 2018-1. *Maest. Interoperability Tools, Desmond Mol. Dyn. Syst.* 2018.
- 719 74. Rivera-Pérez, W.A.; Yépes-Pérez, A.F.; Martínez-Pabón, M.C. Molecular docking and in silico studies of
720 the physicochemical properties of potential inhibitors for the phosphotransferase system of
721 *Streptococcus mutans*. *Arch. Oral Biol.* **2019**, *98*, 164–175, doi:10.1016/j.archoralbio.2018.09.020.
- 722 75. Banerjee, P.; Eckert, A.O.; Schrey, A.K.; Preissner, R. ProTox-II: A webserver for the prediction of toxicity
723 of chemicals. *Nucleic Acids Res.* **2018**, *46*, W257–W263, doi:10.1093/nar/gky318.
- 724 76. Pfizer Inc *Material Safety Data Sheet Material Safety Data Sheet*; 2012;
- 725 77. Chen, D.; Oezguen, N.; Urvil, P.; Ferguson, C.; Dann, S.M.; Savidge, T.C. Regulation of protein-ligand
726 binding affinity by hydrogen bond pairing. *Sci. Adv.* **2016**, *2*, doi:10.1126/sciadv.1501240.
- 727 78. BIOVIA, D. Discovery Studio Modeling Environment, Release 2017, San Diego: DassaultSystèmes, 2016.
728 Adres <http://accelrys.com/products/collaborative-science/biovia-discoverystudio/visualization> download. *php*
729 **2016**.
- 730 79. Pettersen, E.F.; Goddard, T.D.; Huang, C.C.; Couch, G.S.; Greenblatt, D.M.; Meng, E.C.; Ferrin, T.E. UCSF
731 Chimera - A visualization system for exploratory research and analysis. *J. Comput. Chem.* **2004**,

- 732 doi:10.1002/jcc.20084.
- 733 80. Daina, A.; Michielin, O.; Zoete, V. SwissADME: A free web tool to evaluate pharmacokinetics, drug-
734 likeness and medicinal chemistry friendliness of small molecules. *Sci. Rep.* **2017**, *7*, 1–13,
735 doi:10.1038/srep42717.
- 736 81. Tao, L.; Tanzer, J.M.; MacAlister, T.J.; Tao, L.; Tanzer, J.M. Transformation Efficiency of EMS-induced
737 Mutants of *Streptococcus mutans* of Altered Cell Shape. *J. Dent. Res.* **1993**, *72*, 1032–1039,
738 doi:10.1177/00220345930720060701.
- 739 82. Chen, L.; Jia, L.; Zhang, Q.; Zhou, X.; Liu, Z.; Li, B.; Zhu, Z.; Wang, F.; Yu, C.; Zhang, Q.; et al. A novel
740 antimicrobial peptide against dental-carries-associated bacteria. *Anaerobe* **2017**, *47*, 165–172,
741 doi:10.1016/j.anaerobe.2017.05.016.
- 742 83. Esberg, A.; Sheng, N.; Mårell, L.; Claesson, R.; Persson, K.; Borén, T.; Strömberg, N. EBioMedicine
743 *Streptococcus Mutans* Adhesin Biotypes that Match and Predict Individual Caries Development.
744 *EBioMedicine* **2017**, *24*, 205–215, doi:10.1016/j.ebiom.2017.09.027.
- 745 84. Van Der Spoel, D.; Lindahl, E.; Hess, B.; Groenhof, G.; Mark, A.E.; Berendsen, H.J.C. GROMACS: Fast,
746 flexible, and free. *J. Comput. Chem.* **2005**, *26*, 1701–1718, doi:10.1002/jcc.20291.

747



© 2020 by the authors. Submitted for possible open access publication under the terms and conditions of the Creative Commons Attribution (CC BY) license (<http://creativecommons.org/licenses/by/4.0/>).

748